Fatigue Crack Growth in Drill Collars Conical Threaded Joints

M. Beghini[1], L. Bertini[1], M. Pagliaro[1] and A. Barishnikov[2]

(1) Dipartimento di Ingegneria Meccanica, Nucleare e della Produzione, Univ. di Pisa
(2) AGIP RIAP. S. Donato Milanese(MI)

ABSTRACT. *The paper is focused on the fatigue crack growth process observed in full scale conical threaded tool joints (TJ) employed to connect the components (Drill Collars (DC), Drill Pipes (DP), Heavy Wall Drill Pipes (HWDP)) of oil drilling batteries. Fatigue is surely the most common failure mechanism for such components. Several full scale tests have been conduced under alternating bending conditions on TJ of two different sizes. Then, different FM models were applied in order to analyse the Stress Intensity Factor distribution along the crack front. The material fatigue crack growth curve was independently determined, based on the results obtained by standard CT specimen, extracted from the component. Such FCG curves were employed, together with FM analysis to predict the crack growth rate and shape evolution in the full scale components, showing fairly good agreement with experimental results.*

INTRODUCTION

Reliable tools for the analysis of cracked structures under fatigue loading are quite important in order to state defects acceptability limits, to estimate residual operating life and to rationally plan inspections. This is particularly true for components, such as oil drilling batteries TJ, which, due to overall dimensions and typical load levels, the propagation phase constitutes a significant fraction of the total fatigue life. In the present paper, the fatigue crack growth process in oil drilling batteries is analysed, taking account of different initiation points.

EXPERIMENTAL ACTIVITIES

Full Scale Tests

Alternating bending fatigue tests were conducted on TJ two different sizes, i.e. NC26 and NC50 (fig. 1). For the tests two purpose designed resonant test frames were employed [1], shown in figure 2. In such frames, the specimen acts as the spring of a one degree-of-freedom vibrating system, whose excitation is provided by two couples of counter-rotating unbalanced masses. The load applied to the specimen was measured by strain gauges controlled by a personal computer.

During the tests, two techniques were employed in order to detect the onset of fatigue crack, such as:

- variation in dynamic amplification factor;
- variation in second to first order harmonic ratio of stress waveform.

In both case, post-mortem analysis revealed that such techniques allowed to detect the presence of a crack having a length of 10 mm.

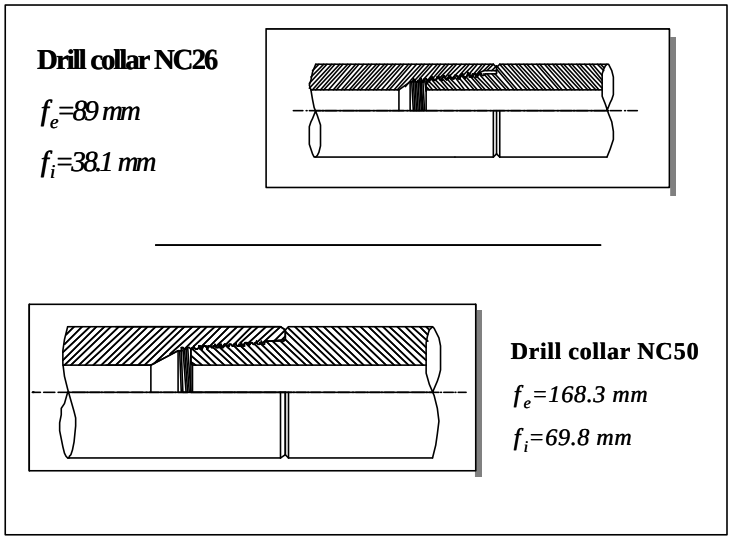

Figure 1. Two different sizes of Drill collar.

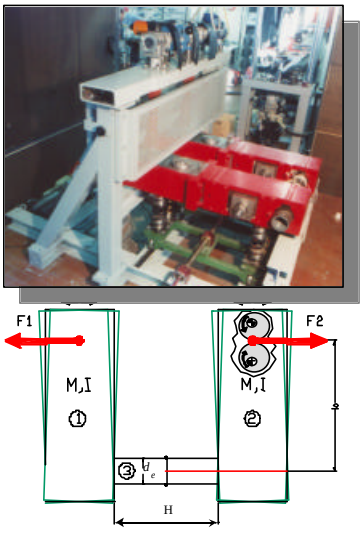

Figure 2. Resonant test device for DC NC26.

Tests were conducted up to complete failure of the specimen or to 10^7 cycles. In a few tests a beach marking technique was applied in order to obtain a registration of subsequent crack fronts.

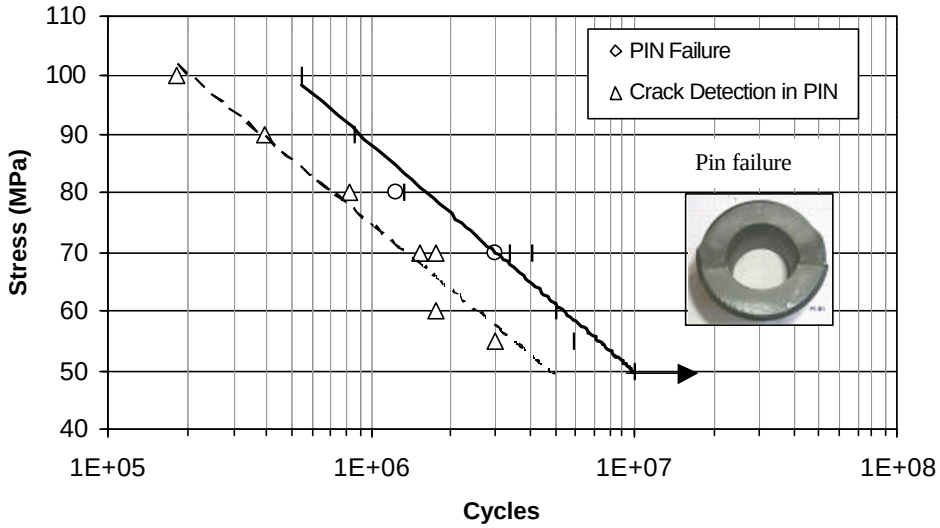

Figure 3. S-N curve for DC NC26.

To this end, applied load was lowered to 30% of test load for 10^4 cycles periods.
Results of full scale tests are reported in Fig. 3. Failure analysis occurred on Pin for NC26 TJ, while it was also observed on Box for NC50 TJ.

Basic Material Characterisation Tests

The following basic material characterisation tests were conducted:

- Tensile tests

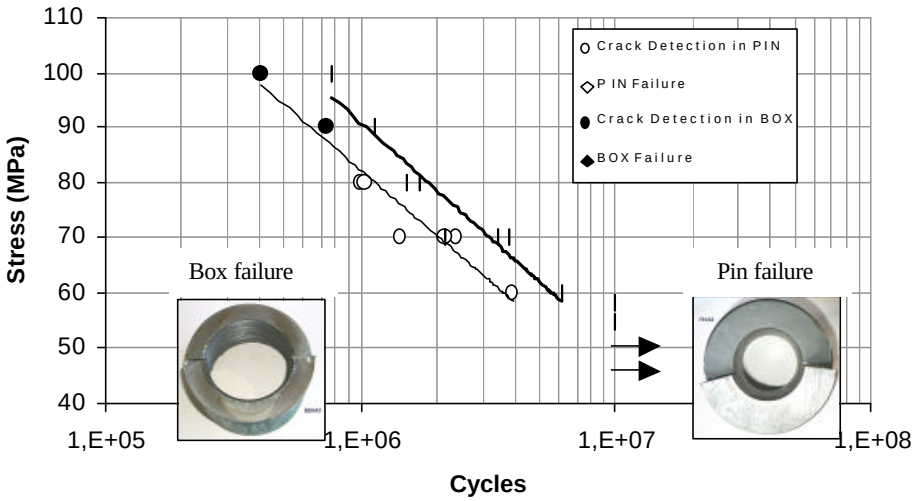

Figure 4. S-N curve for DC NC50.

- Alternating tension compression fatigue tests
- Fatigue tests with non zero mean stress (tensile and compressive)
- Fatigue tests on notched specimens (for notch sensitivity analysis)
- Faigue tests on specimens with different surface finish.

The results of these tests were employed, together with finite element (FE) analysis to predict actual cycles for crack initiation in TJ.

EXPERIMENTAL OBSERVATIONS ON FATIGUE CRACK GROWHT

In few tests a beach marking technique was employed to determine subsequent crack front. Figure 6 shows the crack fronts of specimen 55VM4 that was subjected to beach marking at 50000 cycles intervals.

The crack front, during propagation, undergoes significant shape variations, passing from the initial semi-elliptical shape to a through crack shape. In the first phase the crack was observed to growth with a constant aspect ratio between depth *a* and semi-amplitude *c* (Fig. 7).

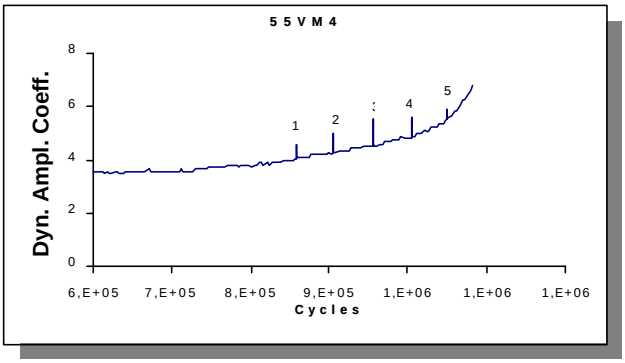

Figure 5. Dynamic Amplification Coefficient.

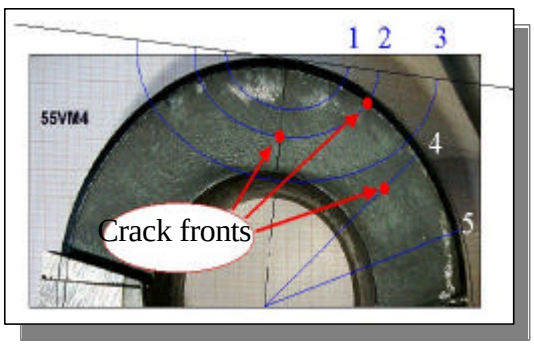

Figure 6. Crack fronts in PIN component.

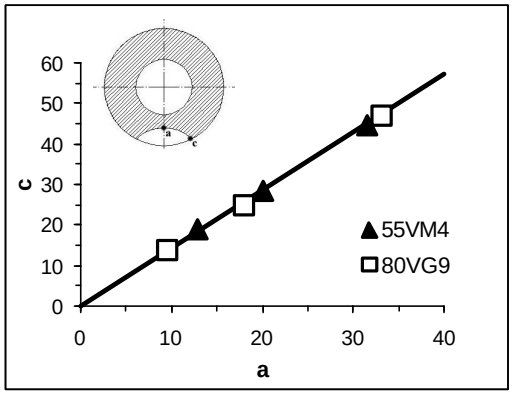

Figure 7. Aspect ratio.

STRESS INTENSITY FACTOR EVALUATION FOR THE PIN

The first phase of the crack propagation was analysed by the model given in [2] for semi-elliptical surface cracks in pipes subjected to either remote tension or bending loads:

$$K_I = \sigma_N \cdot \sqrt{\pi \frac{a}{Q}} \cdot F \tag{1}$$

with:

$$Q = 1 + 1.464 \cdot \left(\frac{a}{c}\right)^{1.65} \tag{2}$$

in which:

- σ_N = bending nominal stress ;
- a and c = main crack dimensions;
- Q = the shape factor for a semi-elliptical crack;
- F = the stress intensity boundary-correction factor.

The second phase of the crack propagation was analyzed by [3],[4] modelling the pipe as a plate with a periodic series of aligned through cracks propagating along the width (Fig.8). For this case , the weight function is available giving by [5] :

$$K_I = f \cdot \sigma \cdot \sqrt{\pi a W} \tag{3}$$

with

$$f = \int_0^a \frac{\sigma(x)}{\sigma} \cdot \frac{m(a,x)}{\sqrt{\pi a}} dx \tag{4}$$

and

$$m(a,x) = \frac{2}{\sqrt{\pi a}} \cdot \cos\left(\frac{\pi x}{2}\right) \cdot \sqrt{\frac{\frac{\pi a}{2}\tan\frac{\pi a}{2}}{\sin^2\frac{\pi a}{2} - \sin^2\frac{\pi x}{2}}} \tag{5}$$

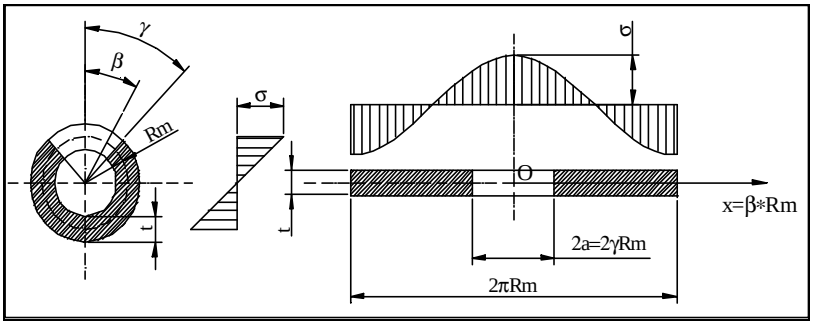

Figure 8. Through crack theory.

STRESS INTENSITY FACTOR EVALUATION FOR THE BOX

The first phase of the crack propagation was analysed by the model given in [6] for a circumferentially cracked pipe with an internal, constant-length, finite-length surface flaw subjected to pure bending loads:

$$K_I = \frac{M}{\pi \cdot R_m^{\,2} \cdot t} F_B(a/t, J/\pi)\sqrt{\pi a} \tag{6}$$

with, according to Article IWB-3650 in Section XI of the ASME Code (1992):

$$F_B(a/t, J/\pi) = 1.1 + \frac{a}{t}\left[-0.09967 + 5.0057\left(\frac{aJ}{t\pi}\right)^{0.565} - 2.8329\left(\frac{aJ}{t\pi}\right)\right] \tag{7}$$

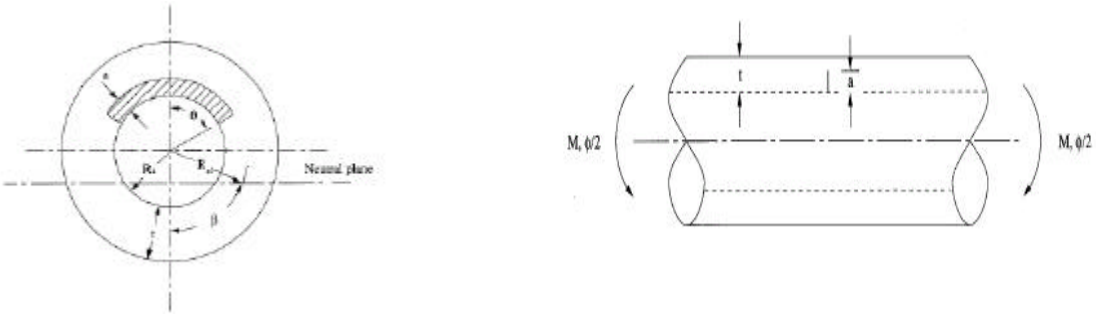

Figure 9. Schematic of surface-cracked pipe geometry and loading.

The second phase of the crack propagation (i.e. after reaching the through crack condition) was analyzed by same model employed for the Pin.

MATERIAL FCG CURVE

Based on experimental crack fronts and on analytical models for SIF evaluation, a series of $\frac{da}{dN}$ - ΔK data points could be obtained. They were fitted with the Priddle equation:

$$\frac{da}{dN} = C\left(\Delta K(\sigma_N, x) - \Delta K_{th}\right)^n \tag{8}$$

The values for the constants are the values found in [3], [4] for a steel AISI 4140 grade E:

$$\Delta K_{th} = 3 \text{ MPa} \quad \text{m}, \; C = 8.888\ 10^{-4}, \; n = 1.92657$$

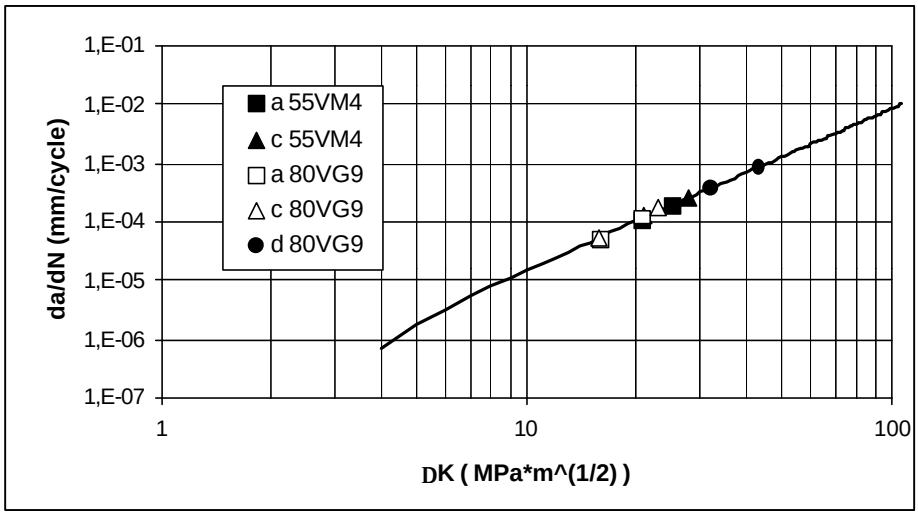

Figure 10. FCG along ΔK for Pin component.

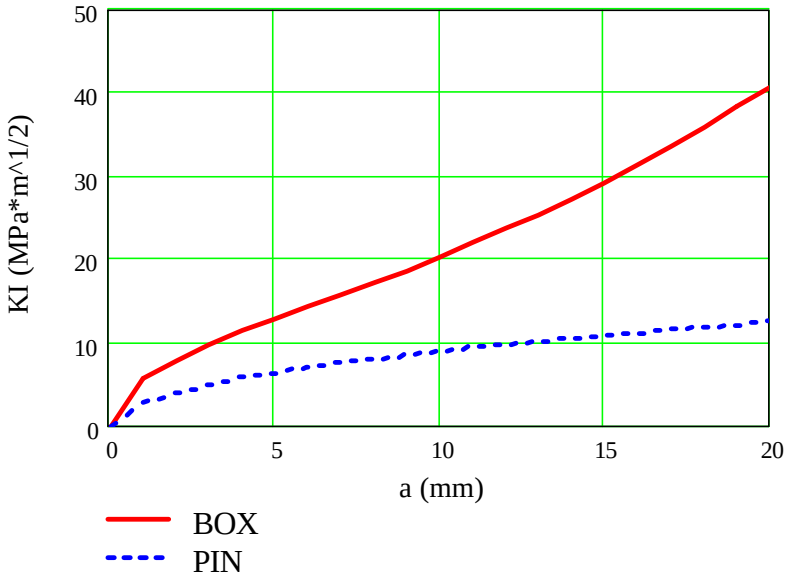

Figure 11. K_I Box and Pin along *a*.

LIFE PREDICTION

The total fatigue life was divided in the sum of three contributions:

$$N_f = N_n + N_{p1} + N_{p2} \tag{9}$$

where

- N_f = cycles to failure;
- N_n = cycles for crack initiation;
- N_{p1} = cycles from initiation, to first detected crack;
- N_{p2} = cycles from first detected to final failure.

Based on basic material characterization and on TJ FE stress analysis, it was possible to estimate N_n.

Then, integrating the equation 8, it was possible to evaluate N_{p1}:

$$\Delta N_p = \int_{l_i}^{l_f} \frac{1}{C \cdot [\Delta K(\sigma_N, x) - \Delta K_{th}]^n} dx \tag{10}$$

The initial crack length l_i was employed as a best fit parameter, obtaining the value = 1 mm, in reasonable agreement with typical upper limits of the "short crack" regime. For l_f the typical value at first detection (i.e. 12 mm was employed).

The predicted and observed cycles for crack initiation and propagation are reported in figure 12 for the Pin and Box.

The agreement with experimental results appear fairly good. It is interesting to observe that propagation life is quite shower in the Box, as compared to the Pin. This can be explained with the different variation of the SIF with crack length in the two cases.

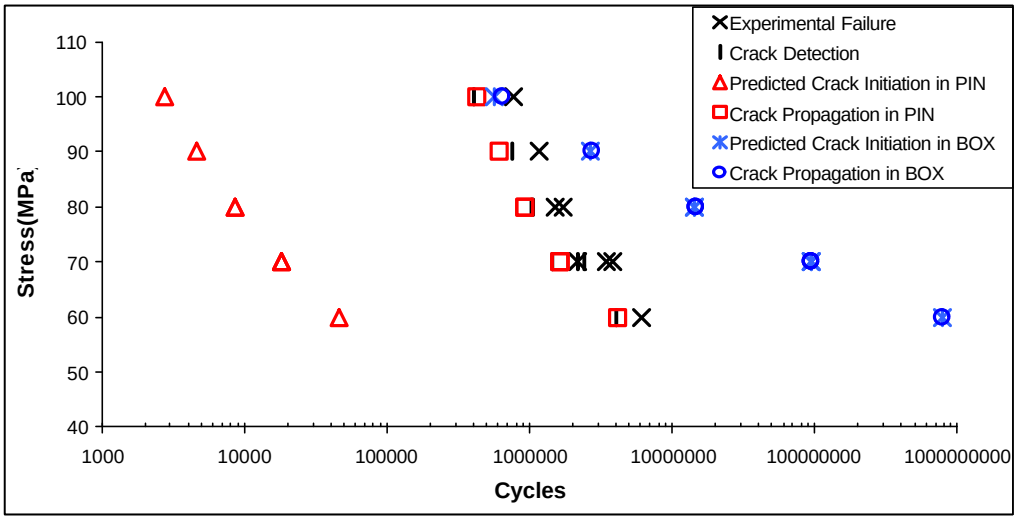

Figure 12. Alternating stress along cycles for Box and Pin.

CONCLUSIONS

The fatigue crack growth process in oil drilling batteries tool joints (TJ) was analysed, showing that it can be satisfactory represented by rather simple fracture mechanics models and by a Paris-like material behaviour. It was also observed that the propagation stage is shorter when fatigue cracks are initiated in the box, rather than when they are initiated in the pin.

REFERENCES

1. Beghini, M., Bertini, L., Frendo, F., Storai, M. and Baryshnikov, A. (1999) Una macchina a risonanza per prove di fatica su particolari cilindrici in piena scala. *Proceedings of XXVII Convegno Nazionale AIAS*, Vicenza, Italy.
2. Raju, I.S. and Newman, J.C. (1986) Stress-Intensity factor for circumferential surface cracks in pipes and rods under tension and bending loads. *Fracture Mechanics: Seventh Volume*, ASTP, STP 905, pp.789-805.
3. Kral, E., Prabir, K., Newlin, S.L. and Quan, S.S. (1984) Fracture mechanics estimate drillpipe fatigue. *Tecnology Oil and Gas Journal*, 6 August 1984.
4. Kral, E., Prabir, K., Newlin, S.L. and Quan, S.S. (1984) Fracture-mechanics concept offers models to help calculate fatigue life in drillpipe. *Tecnology Oil and gas Journal*, 13 August 1984.
5. Wu, X.R. and Carlsson, A.J. (1991) *Weight function and stress intensity factor solutions*. Pergamon Press, Oxford.
6. Rahman, S. and Brust, F.W. (1997) Approximate methods for predicting J-integral of a circumferentially surface-cracked pipe subject to bending. *International Journal of Fracture* **85**, 111-130.